

Rare Earth Coordination Polymers with Zeolite Topology Constructed from 4-Connected Building Units

Xiaodan Guo, Guangshan Zhu,* Zhongyue Li, Yan Chen, Xiaotian Li, and Shilun Qiu*

State Key Laboratory of Inorganic Synthesis & Preparative Chemistry, Jilin University, Changchun 130012, China

Received January 19, 2006

A series of rare earth coordination polymers, $M(\text{BTC})(\text{DMF})(\text{DMSO})$ ($M = \text{Tb}$ (1), Ho (2), Er (3), Yb (4), Y (5)), with zeolite ABW topology have been synthesized under mild conditions. They exhibit the same three-dimensional (3D) architecture and crystallize in monoclinic symmetry space group $P2_1/n$. Their structures are built up from inorganic and organic 4-connected building units, whose vertex symbols are 4·4·6·6·6·8. The building units link to each other to generate approximate $5 \times 8 \text{ \AA}^2$ channels along the [100] direction. The luminescent and magnetic properties of these compounds are investigated, and the results reveal that they could be anticipated to be potential antiferromagnetic and fluorescent materials.

Introduction

Inorganic–organic hybrid coordination polymers with rigid and open frameworks have received intense attention for their intriguing molecular topologies and great potential applications as functional materials.¹ Although many efforts have been made to assemble designed and predictable frameworks and properties, it is still regarded as an effective and successful synthetic strategy to carefully choose functional metal centers and expand the topological networks of inorganic materials.² The structures of many minerals, such as diamond, quartz, rutile, perovskite, PtS, and feldspar, have been artificially produced by replacing monatomic anions (O^{2-} , S^{2-}) with polyatomic organic ligands as linkers and utilizing the well-defined coordination geometries of metal centers as nodes.³ Compared with these inorganic materials, coordination polymers with zeolite topologies are still unexplored.⁴ Recently, our group are engaged in assembling novel frameworks with zeolite topologies through finding suitable organic ligands and represent a novel three-dimensional (3D) compound with the zeolite MTN topology with 2522 \AA^3 cages via consideration of the hexamethylene-

tetramine (hmt) ligand as the meta–organic tetrahedral building block.^{4a} The rare earth ions are always thought to be unsuitable for four-connected nodes because they have a higher coordination number and a more flexible coordination geometry than traditional metals.⁵ However, the amazing optical and magnetic properties of rare earth elements encourage us to explore their coordination fashions.⁶ We find that most rare earth ions of coordination polymers have terminal coordinated molecules, which decrease their coordination number linked with organic ligands, and disassociation or removal of the terminal coordinated molecules from rare earth ions could make them become Lewis acid sites, which may reveal their potential uses as sensors or catalysts

* To whom correspondence should be addressed. E-mail: sqiu@mail.jlu.edu.cn (S. Q.); zhugs@mail.jlu.edu.cn. Fax: (+86) 431 5168331 (S. Q.).

- (1) (a) Seo, J. S.; Whang, D.; Lee, H.; Jun, S. I.; Oh, J.; Jeon, Y. J.; Kim, K. *Nature* **2000**, *404*, 982. (b) Chen, B.; Eddaoudi, M.; Hyde, S. T.; O'Keeffe, M.; Yaghi, O. M. *Science* **2001**, *291*, 1021. (c) Sato, O.; Iyoda, T.; Fujishima, A.; Hashimoto, K. *Science* **1996**, *271*, 49. (d) Kahn, O.; Martinez, C. *Science* **1998**, *279*, 44.
- (2) (a) O'Keefe, M.; Eddaoudi, M.; Li, H.; Reineke, T. M.; Yaghi, O. M. *J. Solid State Chem.* **2000**, *152*, 3. (b) Kim, J.; Chen, B.; Reineke, T. M.; Li, H.; Eddaoudi, M.; Moler, D. B.; O'Keeffe, M.; Yaghi, O. M. *J. Am. Chem. Soc.* **2001**, *123*, 8239.

- (3) (a) Sun, J. Y.; Weng, L. H.; Zhou, Y. M.; Chen, J. X.; Chen, Z. X.; Liu, Z. C.; Zhao, D. Y. *Angew. Chem., Int. Ed.* **2002**, *41*, 4471. (b) Hoskins, B. F.; Robson, R. *J. Am. Chem. Soc.* **1990**, *112*, 1546. (c) Gable, R. W.; Houskins, B. F.; Robson, R. *J. Chem. Soc., Chem. Commun.* **1990**, 762. (d) Chen, B.; Eddaoudi, M.; Reineke, T. M.; Kampf, J. W.; O'Keeffe, M.; Yaghi, O. M. *J. Am. Chem. Soc.* **2000**, *122*, 11559. (e) Eddaoudi, M.; Kim, J.; O'Keeffe, M.; Yaghi, O. M. *J. Am. Chem. Soc.* **2002**, *124*, 376. (f) Rosi, N. L.; Eddaoudi, M.; Kim, J.; O'Keeffe, M.; Yaghi, O. M. *Angew. Chem.* **2002**, *114*, 294.
- (4) (a) Fang, Q. R.; Zhu, G.; Xue, M.; Sun, J. Y.; Wei, Y.; Qiu, S.; Xu, R. *Angew. Chem., Int. Ed.* **2005**, *44*, 2. (b) Tian, Y. Q.; Cai, C. X.; Ji, Y.; You, X. Z.; Peng, S. M.; Lee, G. H. *Angew. Chem., Int. Ed.* **2002**, *41*, 1384. (c) Férey, G.; Serre, C.; Mellot-Draznieks, C.; Millange, F.; Surblé, S.; Dutour, J.; Margiolaki, I. *Angew. Chem.* **2004**, *116*, 6456.
- (5) (a) Kiritsis, V.; Michaelides, A.; Skoulika, S.; Golhen, S.; Ouahab, L. *Inorg. Chem.* **1998**, *37*, 3407. (b) Long, D. L.; Blake, A. J.; Champness, N. R.; Schroder, M. *Chem. Commun.* **2000**, 1369. (c) Long, D. L.; Blake, A. J.; Champness, N. R.; Wilson, C.; Schroder, M. *J. Am. Chem. Soc.* **2001**, *123*, 3401. (d) Wang, Z.; Jin, C. M.; Shao, T.; Li, Y. Z.; Zhang, K. L.; Zhang, H. T.; You, X. Z. *Inorg. Chem. Commun.* **2002**, *5*, 642.

Table 1. Crystallographic Data for Complexes 1–5

	1	2	3	4	5
empirical formula	C ₁₄ H ₁₆ TbNO ₈ S	C ₁₄ H ₁₆ HoNO ₈ S	C ₁₄ H ₁₆ ErNO ₈ S	C ₁₄ H ₁₆ YbNO ₈ S	C ₁₄ H ₁₆ YNO ₈ S
fw	517.2	523.3	525.6	531.4	447.2
cryst syst	monoclinic	monoclinic	monoclinic	monoclinic	monoclinic
space group	<i>P</i> 2 ₁ / <i>n</i>	<i>P</i> 2 ₁ / <i>n</i>	<i>P</i> 2 ₁ / <i>n</i>	<i>P</i> 2 ₁ / <i>n</i>	<i>P</i> 2 ₁ / <i>n</i>
<i>a</i> (Å)	10.8724(11)	10.844(2)	10.8158(9)	10.782(2)	10.8388(12)
<i>b</i> (Å)	15.6218(17)	15.585(3)	15.5514(11)	15.510(3)	15.5918(18)
<i>c</i> (Å)	10.9924(11)	10.961(2)	10.9331(9)	10.881(2)	10.9421(13)
β (deg)	100.702(2)	100.557(2)	100.557(2)	100.26(3)	100.513(2)
<i>V</i> (Å ³)	1834.5(3)	1821.1(6)	1807.8(3)	1790.4(6)	1818.1(4)
<i>Z</i>	4	4	4	4	4
<i>T</i> (K)	293(2)	293(2)	293(2)	293(2)	293(2)
λ (Å)	0.71073	0.71073	0.71073	0.71073	0.71073
ρ_{calcd} (g cm ⁻³)	1.873	1.909	1.931	1.971	1.634
μ (mm ⁻¹)	4.008	4.499	4.797	5.380	3.362
<i>R</i> ^a (<i>I</i> > 20 σ (<i>I</i>))	0.0532	0.0418	0.0454	0.0239	0.0523
<i>R</i> _w ^b	0.1001	0.0872	0.0787	0.0602	0.0876

$$^a R = \sum ||F_o| - |F_c|| / \sum |F_o|. \quad ^b R_w = [\sum w(F_o^2 - F_c^2) / \sum w(F_o^2)]^{1/2}.$$

for organic transformations.⁷ The 1,3,5-benzenetricarboxylic acid (H₃BTC) possesses three carboxylic groups with multifarious coordination modes and could be regarded as a good candidate for an organic four-connected node (Figure S1 in Supporting Information).⁸ In this paper, we reported a series of 3D coordination polymers with ABW zeolite topology, M(BTC)(DMF)(DMSO) (M = Tb (**1**), Ho (**2**), Er (**3**), Yb (**4**), Y(**5**)). Each metal center of these structures, connected with four ligands (BTC), is regarded as an inorganic four-connected node (T1), and a phenyl group of a BTC ligand is considered to be an organic four-connected node (T2) because of its linking with four metal centers. These frameworks contain 5 × 8 Å² channels viewed along the [110] direction. The photoluminescent properties, magnetic properties, and thermal stabilities of these compounds are investigated.

Experimental Section

All chemicals purchased were of reagent grade or better and were used without further purification. Rare earth nitrate salts (M(NO₃)₃·*n*H₂O) were prepared by dissolving rare earth oxides with 6 M HNO₃, while adding H₂O₂ for Tb₄O₇; the mixtures were then evaporated at 100 °C until the crystal film formed. Fluorescence spectroscopy data were recorded on a LS55 luminescence spectrometer. The elemental analyses were carried out on a Perkin-Elmer 240C elemental analyzer. The infrared (IR) spectra were recorded (400–4000 cm⁻¹ region) on a Nicolet Impact 410 FTIR spectrometer using KBr pellets. TGA (thermal gravimetric analyses) were performed under oxygen with a heating rate of 10 °C/min using a Perkin-Elmer TGA 7 thermogravimetric analyzer.

- (6) (a) Liu, W. S.; Jiao, T. Q.; Li, Y. Z.; Liu, Q. Z.; Tan, M. Y.; Wang, H.; Wang, L. F. *J. Am. Chem. Soc.* **2004**, *126*, 2280. (b) Ma, B. Q.; Zhang, D. S.; Gao, S.; Jin, T. Z.; Yan, C. H.; Xu, G. X. *Angew. Chem., Int. Ed.* **2002**, *39*, 3644. (c) Serre, C.; Stock, N.; Bein, T.; Férey, G. *Inorg. Chem.* **2004**, *43*, 3159. (d) Mancino, G.; Ferguson, A. J.; Beeby, A.; Long, N. J.; Jones, T. S. *J. Am. Chem. Soc.* **2005**, *127*, 524. (f) Guo, X.; Zhu, G.; Fang, Q.; Xue, M.; Tian, G.; Sun, J.; Li, X.; Qiu, S. *Inorg. Chem.* **2004**, *44*, 3850.
- (7) (a) Reineke, T. M.; Eddaoudi, M.; Fehr, M.; Kelley, D.; Yaghi, O. M. *J. Am. Chem. Soc.* **1999**, *121*, 1651. (b) Reineke, T. M.; Eddaoudi, M.; O'Keeffe, M.; Yaghi, O. M. *Angew. Chem., Int. Ed.* **1999**, *38*, 2590.
- (8) (a) Devic, T.; Serre, C.; Audebrand, N.; Marrot, J.; Férey, G. *J. Am. Chem. Soc.* **2005**, *127*, 12788. (b) Zhang, Z. H.; Shen, Z. L.; Okamura, T.; Zhu, H. F.; Sun, W. Y.; Ueyama, N. *Cryst. Growth Des.* **2005**, *5*, 1191. (c) Zhang, Z. H.; Okamura, T.; Hasegawa, Y.; Kawaguchi, H.; Kong, L. Y.; Sun, W. Y.; Ueyama, N. *Inorg. Chem.* **2005**, *44*, 6215.

Synthesis of Tb(BTC)(DMF)(DMSO) (1). Tb(NO₃)₃·*n*H₂O (40 mg, 0.10 mmol) and H₃BTC (10 mg, 0.05 mmol) was dissolved in *N,N'*-dimethylformamide (DMF) (10 mL) and dimethylsulfoxide (DMSO) (5 mL) at room temperature in a 50 mL beaker. The beaker was sealed and left undisturbed at 60 °C for 7 days to give colorless crystals. Yield: 72%. Anal. Calcd for C₁₄H₁₆TbNO₈S (517.3): C, 32.51; H, 3.12; N, 2.71. Found: C, 33.48; H, 3.18; N, 2.77.

Synthesis of Ho(BTC)(DMF)(DMSO) (2). The procedure was the same as that for **1** except that Tb(NO₃)₃·*n*H₂O was replaced by Ho(NO₃)₃·*n*H₂O (40 mg, 0.1 mmol). Yield: 77%. Anal. Calcd C₁₄H₁₆HoNO₈S (523.3): C, 32.14; H, 3.08; N, 2.68. Found: C, 32.08; H, 3.06; N, 2.26.

Synthesis of Er(BTC)(DMF)(DMSO) (3). The procedure was the same as that for **1** except that Tb(NO₃)₃·*n*H₂O was replaced by Er(NO₃)₃·*n*H₂O (40 mg, 0.1 mmol). Yield: 75%. Anal. Calcd C₁₄H₁₆ErNO₈S (525.6): C, 31.99; H, 3.07; N, 2.66. Found: C, 31.88; H, 3.06; N, 2.66.

Synthesis of Yb(BTC)(DMF)(DMSO) (4). The procedure was the same as that for **1** except that Tb(NO₃)₃·*n*H₂O was replaced by Yb(NO₃)₃·*n*H₂O (40 mg, 0.1 mmol). Yield: 68%. Anal. Calcd C₁₄H₁₆YbNO₈S (531.4): C, 31.64; H, 3.03; N, 2.64. Found: C, 32.01; H, 3.06; N, 2.66.

Synthesis of Y(BTC)(DMF)(DMSO) (5). The procedure was the same as that for **1** except that Tb(NO₃)₃·*n*H₂O was replaced by Y(NO₃)₃·*n*H₂O (40 mg, 0.1 mmol). Yield: 58%. Anal. Calcd C₁₄H₁₆YNO₈S (447.2): C, 37.60; H, 3.61; N, 3.13. Found: C, 37.51; H, 3.66; N, 3.16.

X-ray Crystallographic Study. The intensity data were collected on a Smart CCD diffractometer with graphite-monochromated Mo K α (λ = 0.71073 Å) radiation at room temperature in the ω -2 θ scan mode. An empirical absorption correction was applied to the data using the SADABS program.⁹ The structures were solved by direct methods. All non-hydrogen atoms were refined anisotropically. Hydrogen atoms were fixed at calculated positions and refined by using a riding mode. All calculations were performed using the SHELXTL program.¹⁰ The crystallographic data were summarized in Table 1, and the selected bond lengths and bond angles of the five complexes were listed in Table 2 and Table S1 in the Supporting Information, respectively.

(9) Sheldrick, G. M. *SADABS, Program for Empirical Absorption Correction for Area Detector Data*; University of Göttingen: Göttingen, Germany, 1996.

(10) Sheldrick, G. M. *SHELXS 97, Program for Crystal Structure Refinement*; University of Göttingen: Göttingen, Germany, 1997.

Table 2. Selected Bond Lengths (Å) for Complexes 1–5

compound 1 ^a			
Tb(1)–O(1)	2.314(4)	Tb(1)–O(2)	2.423(5)
Tb(1)–O(3)	2.426(5)	Tb(1)–O(4)	2.422(4)
Tb(1)–O(5)	2.469(4)	Tb(1)–O(6)#1	2.260(5)
Tb(1)–O(7)	2.350(5)	Tb(1)–O(8)	2.386(5)
compound 2 ^b			
Ho(1)–O(1)	2.300(3)	Ho(1)–O(2)#1	2.235(4)
Ho(1)–O(3)#3	2.444(3)	Ho(1)–O(4)#3	2.398(3)
Ho(1)–O(5)#2	2.405(4)	Ho(1)–O(6)#2	2.398(4)
Ho(1)–O(7)	2.334(4)	Ho(1)–O(8)	2.365(4)
compound 3 ^c			
Er(1)–O(1)	2.279(5)	Er(1)–O(2)#1	2.222(5)
Er(1)–O(3)#3	2.438(5)	Er(1)–O(4)#3	2.386(5)
Er(1)–O(5)#2	2.393(5)	Er(1)–O(6)#2	2.385(5)
Er(1)–O(7)	2.341(5)	Er(1)–O(8)	2.307(6)
compound 4 ^d			
Yb(1)–O(1)	2.363(3)	Yb(1)–O(2)	2.427(3)
Yb(1)–O(3)	2.367(3)	Yb(1)–O(4)	2.375(3)
Yb(1)–O(5)	2.202(3)	Yb(1)–O(6)	2.265(3)
Yb(1)–O(7)	2.290(3)	Yb(1)–O(8)	2.330(3)
compound 5 ^e			
Y(1)–O(1)	2.292(2)	Y(1)–O(2)#1	2.230(3)
Y(1)–O(3)#2	2.447(2)	Y(1)–O(4)#2	2.392(3)
Y(1)–O(5)#3	2.398(3)	Y(1)–O(6)#3	2.396(3)
Y(1)–O(7)	2.358(3)	Y(1)–O(8)	2.312(3)

^a Symmetry transformations used to generate equivalent atoms: #1 $-x + 2, -y, -z + 1$. ^b Symmetry transformations used to generate equivalent atoms: #1 $-x + 2, -y, -z + 2$; #2 $x + 1/2, -y + 1/2, z + 1/2$; #3 $x + 1, y, z$. ^c Symmetry transformations used to generate equivalent atoms: #1 $-x + 1, -y, -z + 1$; #2 $x - 1/2, -y + 1/2, z - 1/2$; #3 $x - 1, y, z$. ^d Symmetry transformations used to generate equivalent atoms: #1 $-x, -y, -z + 1$; #2 $x - 1, y, z$; #3 $x - 1/2, -y + 1/2, z - 1/2$.

Results and Discussion

Complexes 1–5 have been successfully synthesized under mild conditions. Single-crystal X-ray diffraction, elemental analysis, and TGA analysis studies performed on compounds 1–5 reveal that they are identical in structure with the formula M(BTC)(DMF)(DMSO) (M = Tb (1), Ho (2), Er (3), Yb (4), or Y (5)).

Crystal Structure. X-ray diffraction studies performed on these compounds reveal that each asymmetric unit contains one eight-coordinated rare earth ion (M^{3+}), one BTC ligand, one coordinated DMF molecule, and one coordinated DMSO molecule without any guest molecule. As shown in Figure 1, each metal center (M^{3+}) is coordinated with six oxygen atoms (O1–O6) from four carboxylate groups of the BTC ligands and two oxygen atoms (O7, O8) from a terminal DMF molecule and a terminal DMSO molecule. The carboxylic O–M, M–O_{DMF}, and M–O_{DMSO} bonds are in the range of 2.222–2.469, 2.229–2.350, and 2.230–2.386 Å, respectively, and all of them are comparable to those reported for other rare earth metal coordination polymers.^{6f,11}

To deeply understand the structures and how the topology is a prototype for frameworks, it would be helpful to explore the connection mode of the metal centers and organic ligands. In the framework, each metal center (M^{3+}) is connected with

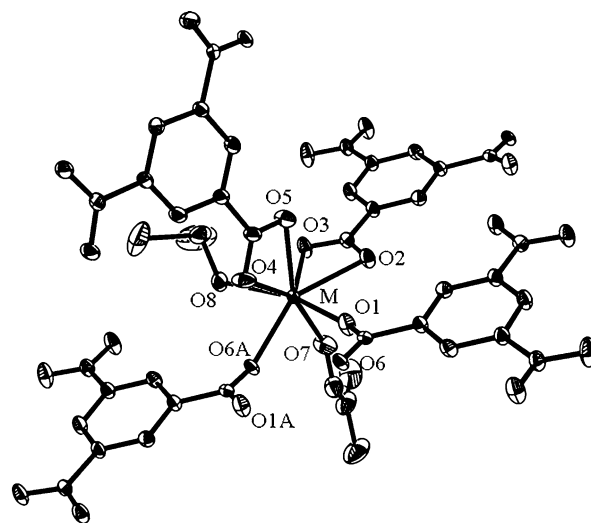


Figure 1. Coordination environments of metal center, M, in M(BTC)-(DMF)(DMSO) (M = Tb (1), Ho (2), Er (3), Yb (4), Y(5)) with non-hydrogen atoms represented by thermal ellipsoids drawn at the 50% probability level. Atoms labeled with additional A are symmetrically equivalent to those atoms without such designation.

four BTC ligands through two chelating bidentate carboxylate groups and two dimondentate carboxylate groups. It is not unreasonable to regard it as an inorganic four-connected node (T1) (Figure 2a). Since each BTC ligand coordinate with four metal centers through carboxylate groups, it is more clear to describe the structure when the phenyl group of the BTC ligand are regarded as an organic four-connected node (T2) (Figure 2b). As seen in Figure 2c, a zeolite ABW topology is given if the couple of four-connected nodes, T1 and T2, are linked each other.¹² The vertex symbols of both T1 and T2 are 4·4·6·6·6·8. As the structure of a zeolite ABW, the framework of compounds also contain eight-membered channels which are formed from four metal centers and four phenyl groups linked by carboxylate groups. Replacement of the four-connected centers of zeolite ABW, Si and Al, with the rare metal ions and phenyl groups replicates and expands the $3.4 \times 3.8 \text{ \AA}^2$ eight-membered channels to approximately $5 \times 8 \text{ \AA}^2$. The channels of the structure are viewed along the [100] direction, as shown in Figure 3.

According to a review by Yaghi's group about the building-block geometries of MOF crystals, there are 31 compounds with the topology of zeolite ABW (also named as **sra**, Al in SrAl_2) in the MOFs with tetrahedral building blocks.¹³ After deeply exploring the structures, we find that all of the building blocks are based on transitional metals, but those based on rare earth metals are still unreported. For the higher coordination number and more flexible coordination geometry of rare earth metals, it is difficult to control the preparation process. A mild synthesis condition and a suitable organic ligand are essential to construct the tetrahedral building units of ABW topology since a mild temperature is helpful for the formation of lower coordination

(11) (a) Wan, Y.; Jin, L.; Wang, K.; Zhang, L.; Zheng, X.; Lu, S. *New J. Chem.* **2002**, 26, 1590. (b) Liu, C. B.; Sun, C. Y.; Jin, L. P.; Lu, S. *Z. New J. Chem.* **2004**, 28, 1019. (c) Sun, H. L.; Gao, S.; Ma, B. Q.; Chang, F.; Fu, W. F. *Micro. Meso. Mater.* **2004**, 73, 89.

(12) *Atlas of Zeolite Framework Types*, 5th ed.; Baerlocher, Ch., Meier, W. M., Olson, D. H., Eds.; Elsevier: New York, 2001.

(13) Ockwig, N. W.; Delgado-Friedrichs, O.; O'Keeffe, M.; Yaghi, O. M. *Acc. Chem. Res.* **2005**, 38, 176.

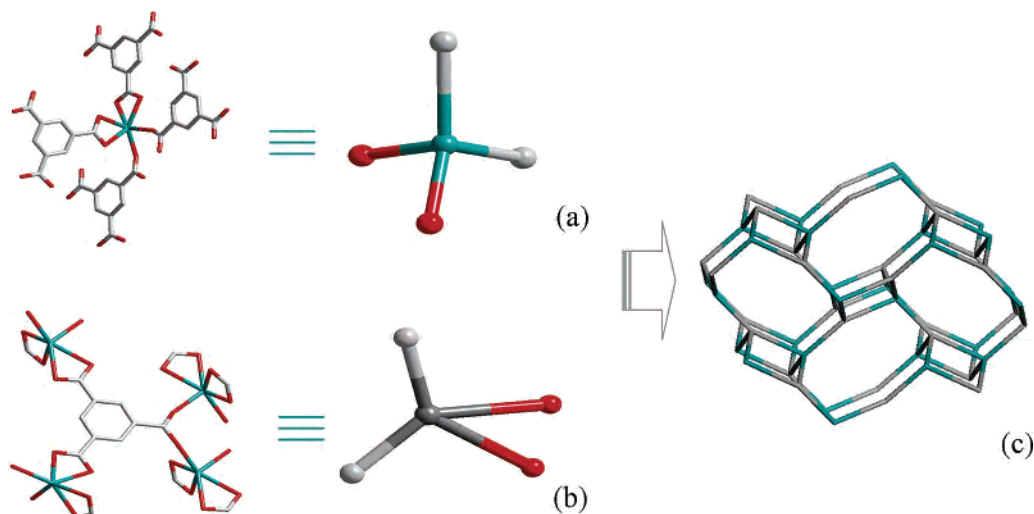


Figure 2. (a) Inorganic four-connected node containing one metal center connected with four BTC ligands and (b) an organic four-connected node presenting one phenyl group linked with four metal centers which link to each other to produce (c) a zeolite ABW topology.

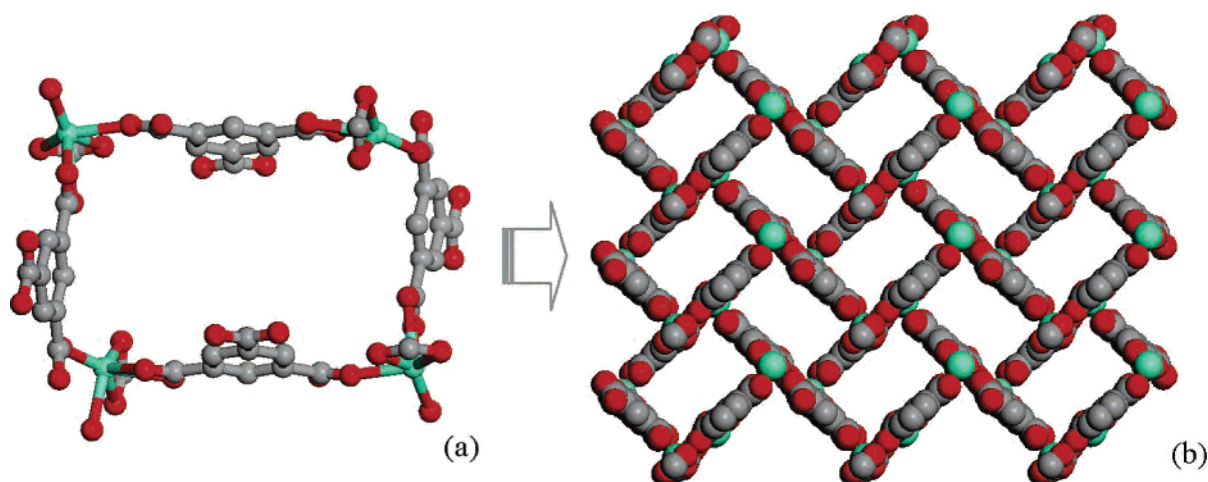


Figure 3. (a) Eight-membered channel consists of four metal centers and four phenyl groups linked through carboxylic groups, and (b) the framework of the compound is viewed along [100] direction.

number rare earth ions and a suitable ligand makes the formation of four-connected nodes possible. So compounds **1–5** are the first with zeolite ABW topology, and the preparation process has been proven effectively to assemble tetrahedral building units to obtain novel structures.

Photoluminescent Properties. The photoluminescent spectra of compound **1** and free H₃BTC are shown in Figure 4. Two emission groups for complex **1** in the range of 350–450 ($\lambda_{\text{ex}} = 235$ nm) and 460–700 nm ($\lambda_{\text{ex}} = 254$ nm) are observed. The emission ranging from 460 to 660 nm is attributed to the terbium ion, corresponding to $^5\text{D}_4 \rightarrow ^7\text{F}_j$ ($J = 6, 5, 4, 3$).¹⁴ Compound **1** exhibits three emission peaks, one blue-shifted emission peak, one red-shifted emission peak, and one main peak without shift compared with that of free H₃BTC. The main emission peak (387 nm) of compound **1** and free H₃BTC may be attributed to $\pi^* \rightarrow n$.¹⁵ The blue-shifted emission band at 363 nm would be assigned to the emission of the ligand-to-metal charge

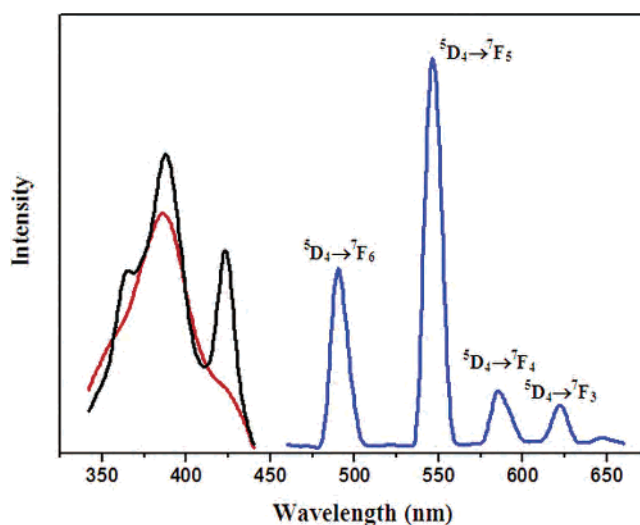


Figure 4. Photoluminescence spectra of (a) Tb(BTC)(DMF)(DMSO) excited at 235 nm, (b) Tb(BTC)(DMF)(DMSO) excited at 254 nm, and (c) H₃BTC excited at 235 nm.

transfer (LMCT).¹⁶ The red-shifted emission peak at 423 nm is probably related to the intraligand fluorescent emission:

(14) Zhao, B.; Chen, X. Y.; Cheng, P.; Liao, D. Z.; Yan, S. P.; Jiang, Z. *H. J. Am. Chem. Soc.* **2004**, *126*, 15394.

(15) Thirumurugan, A.; Natarajan, S. *Dalton Trans.* **2004**, 2923.

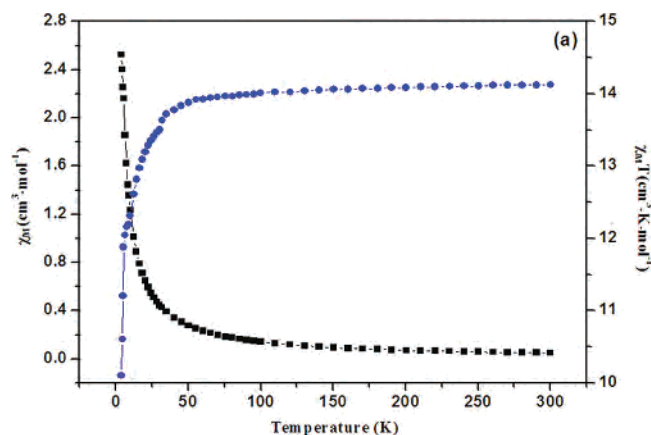


Figure 5. χ_M vs T plot (black) and $\chi_M T$ vs T (blue) plots for Ho(BTC)(DMF)(DMSO).

similar red shifts have been observed before.¹⁷ The photoluminescent spectra of compounds **2**, **3**, **4**, and **5** are investigated and also show blue-emissions, as shown in Figure S2 in Supporting Information. These compounds could be anticipated as potential fluorescent materials.

Magnetic Properties. The magnetic properties of compounds **2** and **3** are investigated from 4 K to room temperature. For compound **2**, the observed value of $\chi_M T$ per [Ho] unit is $14.12 \text{ cm}^3 \text{ K mol}^{-1}$ at room temperature, which is close to the value of two noninteracting Ho^{3+} in the $^5\text{I}_8$ ground state.¹⁸ With a decrease in the temperature, $\chi_M T$ decreases smoothly to a minimum of $10.10 \text{ cm}^3 \text{ K mol}^{-1}$ at 4 K. The plot of χ_M^{-1} versus T over the whole temperature range obeys the Curie–Weiss law [$\chi = C/(T - \theta)$] with $C = 13.87 \text{ cm}^3 \text{ K mol}^{-1}$ and $\theta = -0.58 \text{ K}$. The decrease of $\chi_M T$ and the negative value of θ indicate that the antiferromagnetic interaction between the Ho^{3+} ions dominates the magnetic properties of complex **2** (Figure 5). The magnetic behavior of compound **3** is represented in Figure S5 in the Supporting Information and shows that $\chi_M T$ increases with increasing temperature over the whole temperature range. At room temperature, $\chi_M T$ is $11.07 \text{ cm}^3 \text{ K mol}^{-1}$, which is slightly lower than the value of Er^{3+} in the $^4\text{I}_{15/2}$ ground state.¹⁷ The plot of χ_M^{-1} versus T also obeys the Curie–Weiss law [$\chi = C/(T - \theta)$] with $C = 11.27 \text{ cm}^3 \text{ K mol}^{-1}$ and $\theta = -6.00 \text{ K}$. So compound **3** displays an antiferromagnetic interaction between the Er^{3+} ions.

Thermal Stability. The thermal stability of compound **1** has been studied using TGA and PXRD at different temperatures. The TGA curve performed from 35 to 800 °C shows no weight loss until 200 °C, which corresponds to the crystallographic result without guest molecule. The first weight loss of 28.58% from 200 to 300 °C is attributed to

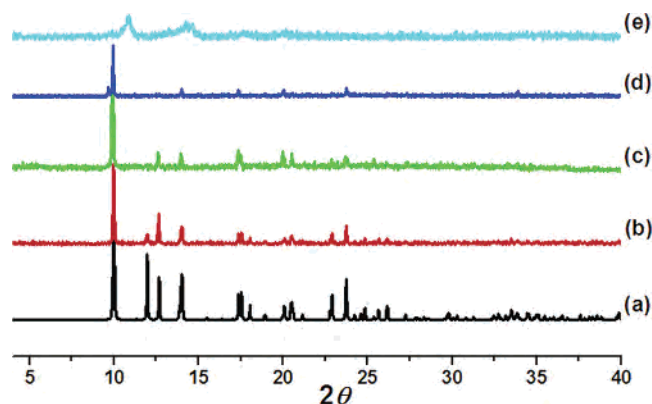


Figure 6. PXRD patterns for Tb(BTC)(DMF)(DMSO): (a) a simulated PXRD pattern calculated from single-crystal structure (black), (b) as-synthesized (red), (c) after being heated at 150 °C (green), (d) after being heated at 200 °C (blue), and (e) after being heated at 250 °C (light blue).

the dissociation of coordinated DMF and DMSO molecules (calculated 29.23%). The decomposition of the compound starts above 450 °C, and the remaining weight of 39.28% corresponds to the percentage of the Tb and O components, Tb_4O_7 (Figure S3 in Supporting Information). The powder X-ray diffractions are performed for the as-synthesized sample, and the samples heated at 150, 200, and 250 °C, respectively (Figure 6). The PXRD patterns for samples heated at 150 and 200 °C are similar to that of as-synthesized sample, which indicates that such temperatures do not lead to an obvious phase transformation. When the sample is heated at 250 °C, the long-range order of the structure is lost and a phase transformation is observed. So, the dissociation of coordinated DMF and DMSO molecules leads to the loss of structure and a phase transformation.

IR Spectrum. The compounds display similar IR spectra. As shown in Figure S4 in Supporting Information, the asymmetric and symmetric stretching vibrations of the carboxylate groups have bands at 1538 and 1396 cm^{-1} . The bands at 1607, 3066, 851, 680, and 771 cm^{-1} are attributed to the aromatic skeleton vibration of benzene ring, $\nu_{\text{C-H}}$ of benzene, $\delta_{\text{C-H}}$ out of the face of benzene, and the 1,4-substitute of benzene ring, respectively. The bands at 1668 and 2929 cm^{-1} are from $\nu_{\text{C=O}}$ and the asymmetric stretching vibration of the methyl group of the DMF molecules. The lack of IR bands at 2657, 2545 (COOH-H), and 1690 cm^{-1} (CCOOH=O) indicates the complete deprotonation of H_3BTC after the reaction. The broad band centered at 3500 cm^{-1} is attributed to the H-bonded $\nu(\text{OH})$ groups mainly from adsorbed water.¹⁹

Conclusions

A series of novel coordination polymers with zeolite ABW topology, $\text{M}(\text{BTC})(\text{DMF})(\text{DMSO})$ ($\text{M} = \text{Tb}$ (**1**), Ho (**2**), Er (**3**), Yb (**4**), Y (**5**)), have been synthesized first through assembling both inorganic and organic building units. Each metal center is regarded as an inorganic four-connected node, for its connection with four BTC ligands. And the phenyl

- (16) (a) Dai, J. C.; Wu, X. T.; Fu, Z. Y.; Cui, C. P.; Hu, S. M.; Du, W. X.; Wu, L. M.; Zhang, H. H.; Sun, R. Q. *Inorg. Chem.* **2002**, *41*, 1391. (b) Zhang, L. Y.; Liu, G. F.; Zheng, S. L.; Ye, B. H.; Zhang, X. M.; Chen, X. M. *Eur. J. Inorg. Chem.* **2003**, 2965.
- (17) (a) Chen, W.; Wang, J. Y.; Chen, C.; Yue, Q.; Yuan, H. M.; Chen, J. S.; Wang, S. N. *Inorg. Chem.* **2003**, *42*, 944. (b) Thirumurugan, A.; Natarajan, S. *Dalton Trans.* **2004**, 2923.
- (18) (a) Benelli, C.; Gatteschi, D. *Chem. Rev.* **2002**, *102*, 2369. (b) Zheng, X.; Wang, Z.; Gao, S.; Liao, F.; Yan, C.; Jin, L. *Eur. J. Inorg. Chem.* **2004**, 2968.

- (19) Fang, Q. R.; Shi, X.; Wu, G.; Tian, G.; Zhu, G. S.; Wang, R. W.; Qiu, S. L. *J. Solid State Chem.* **2003**, *176*, 1.

groups of BTC ligands are considered as organic four-connected nodes because they are linked with four metal centers. The building units link to each other to lead to a three-dimensional framework with approximate $5 \times 8 \text{ \AA}^2$ channels along the [100] direction. Compound **1** exhibits the characteristic emission of terbium ions, and all of these compounds show blue emissions. Compounds **2** and **3** display antiferromagnetic interactions. Thus, these compounds could be anticipated as potential antiferromagnetic and fluorescent materials.

Acknowledgment. This work was funded by the State Basic Research Project (G2000077507) and the National Nature Science Foundation of China (Grants 20571030, 20531030, 29873017, 20273026, and 20101004).

Supporting Information Available: CIF files, selected bond lengths and angles, and emission spectra. This material is available free of charge via the Internet at <http://pubs.acs.org>.

IC060116H